

THIRTEENTH EUROPEAN ROTORCRAFT FORUM

74
Paper No. 60

SIMULATION MODELS FOR OPTIMIZATION OF HELICOPTER
TAKEOFF AND LANDING

T. CERBE, G. REICHERT

TECHNICAL UNIVERSITY OF BRAUNSCHWEIG
BRAUNSCHWEIG, GERMANY

September 8-11, 1987

ARLES, FRANCE

SIMULATION MODELS FOR OPTIMIZATION OF HELICOPTER TAKEOFF AND LANDING

T. Cerbe
G. Reichert

Technical University of Braunschweig
Braunschweig, Germany

Abstract

The application of simulation models for helicopter takeoff and landing is of great interest for different problems. This is for example the calculation of helicopter takeoff and landing performances during the development phase, the analytical determination of performances for certification in support of experimental determination from flight test data and the optimization of helicopter takeoff and landing for certificated helicopters.

The problematical nature of helicopter takeoff and landing will be discussed for selected procedures. Simulation models with different complexity for determining takeoff and landing flight-paths will be presented and verified through flight tests. On the basis of parameter variation the influence of essential parameters on takeoff and landing performances will be shown by means of simulation results.

Notation

F	thrust
g	gravity constant
G	gross weight
H, H_{IGE}	height, ground effect height
I	moment of inertia
\underline{I}_f	inertia matrix
K_G	weight coefficient $K_G = \frac{2G}{\rho U^2 S}$
K_P	power coefficient $K_P = \frac{2P}{\rho U^3 S}$
\underline{K}	force vector
L, M, N	roll-, pitch-, yaw-moment
m	helicopter mass
\underline{M}	moment vector
\underline{M}_{fg}	transformation matrix, geodetic axis to body axis
M_R, M_{TR}	rotor-, tail rotor-torque
p, q, r	rate of roll, pitch and yaw in body axis

P	power
$P_{av.}, P_{req.}$	power available, power required
P_i	induced power
$P_{aux.}$	auxiliary power
R	rotor radius
s_S, s_L	takeoff-, landing-distance
S	rotor disc area
t	time
u, v, w,	airspeed components
U	rotor tip speed $U=R \cdot \omega$
V	airspeed
\underline{V}_{Kf}	flight path velocity vector in body axis
\underline{V}_{Kg}	flight path velocity vector in geodetic axis
V_Y	airspeed of maximum rate of climb
V_{TOSS}, V_{BLSS}	takeoff-, balked landing- safety speed
w_i	induced velocity
w_{ih}	induced velocity in hover
X, Y, Z	forces
Z_R	rotor height above ground
α	angle of attack
ϕ, θ, ψ	flight attitude angle
X	flight path azimuth
Y	flight path angle
$\delta_{OR}, \delta_{OTR}$	collective pitch for rotor and tail rotor
δ_C	lateral pitch
δ_S	longitudinal pitch
θ'	resultant flow angle (source model)
σ	solidity
ρ	air density
ω_R, ω_{TR}	angular velocity of rotor and tailrotor
$\underline{\Omega}_f$	angular velocity vector in body axis
AEO	all engines operating
CDP	critical decision point
IGE	in ground effect
LDP	landing decision point
OGE	out ground effect
OEI	one engine inoperative

1. Introduction

Due to its particular aerodynamic and flightmechanic design, the helicopter has the capability, to perform takeoff and landing by different procedures. In dependence of helicopter performances, takeoff and landing area and registration category one of these procedures is used.

Takeoff and landing procedures are defined in the FAR (Federal Aviation Regulations) of the FAA (Federal Aviation Administration) /1/, /2/. Apart from normal takeoff and landing, according to FAR Part 27 and Part 29 Cat. B, takeoff and landing procedures according to Part 29 Cat. A are of special importance. These procedures require continued takeoff with a safe climbout in event of engine failure.

Up to now there do not exist but few theoretical investigations concerning performances of helicopter takeoff and landing. The determination of performances during takeoff and landing is mainly obtained by flight tests, as calculations still cause difficulties because of the required accuracy. So the performances characteristical for takeoff and landing have to be proved by flight test during certification. The certification of helicopters is desirable basing on calculated evidence of performances and some flight tests in addition.

Besides the evidence of performances for certification, the prediction of takeoff and landing performances during the development of helicopters as well as the optimization of takeoff and landing procedures is of special interest. So far, only a few studies exist dealing with optimization of normal takeoff /3/. For normal landing and the Cat. A procedures, however, which become more and more important, investigations for optimization purposes are not known. This mainly results from the lack of suitable analytical methods for computing takeoff and landing.

The request for improved analytical methods results from considerations relating to safety and economic efficiency. On the one hand flight tests for takeoff and landing are critical tests concerning safety reaching the limits of the flight envelope, and on the other they are time-consuming and costly tests.

Improved analytical methods computing helicopter performances for takeoff and landing require an increased accuracy in calculation of power required and power available. Power excess, power deficiency, respectively, are relevant for the possible rate of climb and descent as well as for the capability of acceleration and deceleration. The ground effect has to be taken into account calculating the power required.

Numerical simulation can be used as an analytical method. For takeoff and landing flight path, translational velocities and accelerations, power required, flight attitude angles and control inputs are of special interest. By means of numerical integration the differential equations of motion of the helicopter will be solved. Particularly for optimization simplified simulation models have to be developed, which need less computation time.

2. Takeoff and Landing Procedures

2.1 Segmental Subdivision of Procedures

The numerical simulation of takeoff and landing procedures necessitates the subdivision of the different procedures into segments. The subdivision and definition of the segments is chosen according to the maneuver /4/. For instance it is obvious to choose climb for takeoff and descent for landing as corresponding segments.

As already mentioned, the Cat. A procedures relating to FAR Part 29 are of special importance apart from the normal procedures. As long as engine failure are not taken into consideration, Cat. A procedures comprise normal procedures. For this reason particulars of normal procedures are not considered when performing the segmental subdivision.

Figure 1 and 2 show segmental subdivision of takeoff and landing procedures Cat. A. With regard to engine failure OEI (one engine inoperative), two cases are of interest: engine failure before and after CDP (critical decision point) and LDP (landing decision point). Borderline case is engine failure within the decision point.

Takeoff begins with hover IGE (in ground effect) at a height H_{IGE} . At transition into forward flight, the helicopter accelerates to decision speed V_{CDP} and climbs to height H_{CDP} . Without engine failure, the takeoff will be continued normally and the climb will be performed at the speed of maximum rate of climb V_y . If one engine fails before CDP, the takeoff has to be finished by emergency landing (rejected takeoff). If one engine fails after CDP, takeoff has to be continued safely with the power available of the operating engine (continued takeoff). A safety height of $H_{min} = 35\text{ft}$ has to be cleared. During transition, the helicopter accelerates to takeoff safety speed V_{TOSS} enabling a minimum rate of climb of $100\text{ft}/\text{min} \approx 0,5\text{m}/\text{s}$.

The length of the different segments depends on the performance capability of the helicopter as well as on the maneuver strategy. For example the first segment can be omitted when the helicopter changes directly from hover to climb. The total takeoff distance is the distance from hover point either to the point, where the height $H_{min} = 35\text{ft}$ is cleared or to the final stop for rejected takeoff. The longer one has to be indicated as required takeoff distance. For calculations it is possible to subdivide the segment for engine failure still more precisely.

The landing procedure, figure 2, is subdivided into two segments. The first one is a descent segment not relevant for the calculation of landing distance. With the LDP generally lying over the 50ft-height the second segment begins, namely the landing segment, bailed landing segment, respectively. If one engine fails before LDP, it is either possible to interrupt the landing (bailed landing) or to continue it. If one engine fails after LDP the landing has to be continued. The landing is finished by the flare resulting in hover at low height IGE or in touch down.

The landing distance without engine failure is taken from the point where the helicopter is at the 50ft-height up to reaching hover. In event of engine failure, the landing distance is taken from the 50ft-height (the corresponding lower height must be chosen) either until reaching the 35ft-height for bal-

ked landing or up to the point where the helicopter comes to a complete stop for continued landing. Usually, the helicopter touches down with a remaining speed, if power available of the operating engine is significantly less than the power required for hover. Here, the longer distance has also to be indicated as landing distance.

2.2 Demands on the Mathematical Model

Generally, a mathematical model has to solve the corresponding problems to be investigated with sufficient accuracy. For this purpose the essential physical effects have to be considered by the model chosen. It should be as complex as necessary and as simple as possible. Comprehensive and complex models are of little practical use when they cannot be applied on today's computers for technical reasons, e.g. due to large computation time. On the other hand models simplified too much, thus neglecting important effects and becoming too inaccurate, are also not recommendable. Therefore, the model to be developed will always be a compromise regarding its complexity.

The statements of the problem to be investigated are limited to performances of takeoff and landing. Questions relating to controllability and stability belonging to the scope of flying qualities will be omitted, provided that performances are not affected. Therefore, it is for instance not required to include the entire dynamic of the helicopter.

Simplistic the following questions are formulated:

- Which flight path basing on determined power available can be flown with and without engine failure?
- What is the power required basing on determined flight path?

Further refined statements of the problem can be derived. Regarding the Cat. A procedures, among others the determination of the decision points CDP and LDP is of special interest. Questions about different variables influencing takeoff and landing distances are of main concern for parameter investigations. Optimization investigations deal with flight path optimization, for instance in the most simple case to minimize takeoff and landing distances. For all problems the calculation of flight path, translational velocities and accelerations as well as power required is needed.

In principle simulation by solving the differential equations of motion of the helicopter numerically gives the necessary information. However, the complete differential equations also describe the coupled modes of the helicopter, which are partly unstable. For considerations regarding performances they are of minor importance. In chapter 3, the simulation model basing on the differential equation of motion is simplified step by step.

Additionally, a simulation model for takeoff and landing must contain a calculation of power required and power available with high accuracy /5/. The calculation of power required is usually founded on computation of the induced velocity at the rotor disc and the blade element theory for computing rotor forces and moments. The ground effect has an essential influence

on the induced velocity. The ground effect has to be considered by an appropriate model for hover and low forward flight. For computing power available as well as further engine variables, an engine calculation has to be made basing for instance on stationary engine data fields.

3. Simulation Models

3.1 Three-Dimensional Simulation Model

Simulating the helicopter means to flightmechanics solving the differential equations of motion. These equations are numerically solved by integration of the translational and rotational accelerations.

The differential equations of motion can be indicated in matrix form:

$$\begin{aligned} m \cdot (\dot{\underline{V}}_{Kf} + \underline{\Omega}_f \times \underline{V}_{Kf}) &= \underline{\Sigma K}_f \\ \underline{I}_f \cdot \dot{\underline{\Omega}}_f + \underline{\Omega}_f \times (\underline{I}_f \cdot \underline{\Omega}_f) &= \underline{\Sigma M}_f \end{aligned} \quad (1)$$

The equations comprise the helicopter forces and moments, which consist of the helicopter's different components as rotor, tail rotor, fuselage and empennage.

After performing the matrix operations, six nonlinear differential equations of the rigid body for the 3D-model (three-dimensional model) are obtained from equation (1):

$$\begin{aligned} m \cdot (\dot{u}_{Kf} + w_{Kf} \cdot q - v_{Kf} \cdot r) &= \Sigma X_f - m \cdot g \cdot \sin \theta \\ m \cdot (\dot{v}_{Kf} + u_{Kf} \cdot r - w_{Kf} \cdot p) &= \Sigma Y_f + m \cdot g \cdot \cos \theta \sin \phi \\ m \cdot (\dot{w}_{Kf} + v_{Kf} \cdot p - u_{Kf} \cdot q) &= \Sigma Z_f + m \cdot g \cdot \cos \theta \cos \phi \\ I_{xx} \cdot \dot{p} - I_{xz} \cdot \dot{r} - I_{xz} \cdot p \cdot q + (I_{zz} - I_{yy}) \cdot q \cdot r &= \Sigma L_f \\ I_{yy} \cdot \dot{q} + I_{xz} \cdot (p^2 - r^2) - (I_{zz} - I_{xx}) \cdot p \cdot r &= \Sigma M_f \\ I_{zz} \cdot \dot{r} - I_{xz} \cdot \dot{p} + I_{xz} \cdot q \cdot r - (I_{xx} - I_{yy}) \cdot p \cdot q &= \Sigma N_f \end{aligned} \quad (2)$$

Figure 3 gives a survey on the components, the coordinate systems as well as the forces and moments. As there are defined different coordinate systems for the components, the forces and moments have to be transformed into the coordinate system fixed at the center of gravity.

The degrees of freedom for the rotor blades of main and tail rotor are added to the degrees of freedom of the rigid body. These are flapping and lagging motion as well as the blade torsion. For performance calculations simplified rotor models, possibly without rotor degrees of freedom are generally sufficient. In the following the rotor will be calculated with and without flapping motion. For this purpose a quasi-stationary flapping motion is considered, i.e. the rotor is in a quasi-stationary state at any time of simulation. The tail rotor is computed without flapping motion.

If the forces and moments are known, the power required can be calculated from the torques of tail and main rotor:

$$P_{\text{req.}} = M_R \cdot \omega_R + M_{\text{TR}} \cdot \omega_{\text{TR}} + P_{\text{aux.}} \quad (3)$$

In this equation the auxiliary power consumption is additionally taken into account.

Computing the forces and moments of the main rotor by means of the blade element theory represents an essential part of the performance calculation. The inflow angle at the blade must be known, which consists of the helicopter's translational and rotational motion, the motion of the rotor blade and the induced velocity.

The calculation of the induced velocity for climb and descent causes problems. The momentum theory can be used as suitable approximation for a certain range of velocities. However, above all in the range of vortex ring state it gives induced velocities deviating from experimentell results. Figure 4 shows results obtained by momentum theory in comparison with experiments for different rates of climb and descent /5/.

The ground effect has an essential influence on the induced velocities and this way on the induced power as well as on the total power required. During takeoff and landing, the helicopter is near the ground, so the ground effect has to be considered. For hover, the ground effect causes an increased thrust at constant power with decreasing distance of the helicopter from ground. For constant thrust, the power required will be reduced. In the low forward flight region the influence of the ground effect decreases with increasing velocity. This effect is superposed by the influence of velocity on the induced power, which does also exist without ground effect. The ground effect can be described by the method of images.

The main principle of the method of images is the mirror-inverted positioning of the fluid dynamic rotor model at the ground. The source model is a relatively simple one, where the rotor is replaced by a source. Figure 5 shows the source model for forward flight IGE. Investigations /6/ have proved that this model mostly corresponds with results achieved by experiments. First of all the model has been developed for the condition of constant induced power, however it can be extended for constant thrust.

According to /7/ for the relation of induced power IGE and induced power OGE at constant thrust is obtained:

$$\left(\frac{P_{i\text{IGE}}}{P_{i\text{OGE}}} \right)_{F=\text{konst}} = \left(\frac{w_{i\text{IGE}}}{w_{i\text{OGE}}} \right)_{F=\text{konst}} = \left(1 - \frac{1}{16} \left(\frac{R}{Z_R} \right)^2 \left(\frac{w_{i\text{OGE}}}{w_{ih,\text{OGE}}} \right)^4 \right)^{\frac{3}{2}} \quad (4)$$

The source model according to equation (4) can be integrated directly into the rotor inflow calculation. The result of a performance calculation is presented in figure 6. The figure shows power required IGE and OGE as a function of forward velocity. The strong decrease of ground effect at increasing velocity is clearly shown.

Figure 7 shows the helicopter IGE at low forward velocity. In front of the helicopter there occurs a ground vortex. At increasing velocity the vortex gets to the back until it disappears behind the helicopter at a medium velocity. Only recent research deals intensively with the ground vortex /8/, /9/, especially with finding out strength and position of the vortex. However, there does not exist any sufficient analytical model describing the ground vortex up to now.

Apart from the calculation of power required, the calculation of power available is of importance. For instance there are two possibilities: On the one hand there is the thermodynamic engine simulation as mostly used by engine manufacturers, and on the other the calculation by engine data fields stated by the manufacturers. The latter requires less computation time. The engine data fields comprise the relevant variables, as engine power available, fuel consumption etc. in dependence of height of pressure altitude, air temperature and power setting as multi-dimensional fields. By multi-dimensional spline interpolation the necessary intermediate data are determined from the data fields.

Simulating the helicopter by the 3D-model requires the control inputs influencing the system helicopter. As a result of the simulation we get the helicopters motion, i.e. the flight state variables and the flight path as a function of time. This kind of simulation is termed "explicite" simulation here. Due to the instabilities of the helicopter an automatic control system or a pilot model will be additionally required.

An essential disadvantage of this kind of simulation is given by the relatively complex task of predetermination of the control input, the design of the automatic control system, respectively, as well as by the fact that the flight path results from the calculation. The simulation for instance of a landing cause difficulties in finding control inputs in a way that the simulation result will be indeed a landing. This task, however, will be complicated because of the helicopter's strong coupling of longitudinal and lateral motion.

Moreover, the large computation time is unfavourable. The 3D-model is not suitable for optimization investigations, calculating with each optimization step one takeoff, one landing, respectively. In the following the 3D-model will be simplified step by step.

3.2 Two-Dimensional Simulation Model

The coupling of longitudinal and lateral motion of the helicopter makes it necessary that maneuvering in the geodetical longitudinal plane basically requires forces and moments in the helicopter-fixed longitudinal and lateral plane. Already in case of stationary forward flight without side slip the flight attitude angles are not equal to zero.

Regarding takeoff and landing in the x_g -/ z_g -plane in direction of the positive x_g -axis, the flight path azimuth X will become zero. Furtheron, idealized flight maneuvers without side slip are supposed and bank angle Φ is assumed equal to zero. It can be shown that the influence of the bank angle on performances is neglectable. With these assumptions the azimuth angle Ψ also becomes zero.

Simultaneously, the angular velocities and accelerations p, r, \dot{p} and \dot{r} can be omitted. The same applies to the lateral translational velocity and acceleration v_{Kf} and \dot{v}_{Kf} . So the equations (1), (2), respectively, can be simplified as follows:

$$\begin{aligned}
 m \cdot (\dot{u}_{Kf} + w_{Kf} \cdot q) &= \Sigma X_f - m \cdot g \cdot \sin \theta \\
 m \cdot (\dot{w}_{Kf} - u_{Kf} \cdot q) &= \Sigma Z_f + m \cdot g \cdot \cos \theta \\
 0 &= \Sigma L_f \\
 I_{yy} \cdot \dot{q} &= \Sigma M_f \\
 0 &= \Sigma N_f
 \end{aligned} \tag{5}$$

These equations describe the two-dimensional motion of the helicopter with three degrees of freedom (two translational and one rotational) and leads to the 2D-model (two-dimensional model). As equations (2) they are partially solved by an "explicite" simulation, i.e. by predetermining control inputs. However, only two control inputs can be predetermined as a function of time, preferably the collective pitch and longitudinal pitch, while the other control inputs, as collective pitch of the tail rotor and the lateral pitch, have to be calculated iteratively from the roll- and yaw-moment equation. These equations cannot be solved explicitly according to control inputs.

Further simplifications lead to the quasi-stationary 2D-dimensional model /4/.

3.3 Quasi-Stationary Two-Dimensional Simulation Model

Angular velocities and accelerations occur only for short time in the transitions of the different takeoff and landing segments. Moreover, the terms of inertia in the moment equations have only small influence on power required. Also aerodynamic forces and moments due to rates of pitch have only a minor effect on power required. However, EULER terms basing on rates of pitch influencing power required have to be taken into consideration (terms $m \cdot w_{Kf} \cdot q$ and $m \cdot u_{Kf} \cdot q$ of equation (5)).

With the transformation of the geodetical accelerations into the body-fixed coordinate system:

$$\frac{d\underline{v}_{Kf}}{dt} = \underline{M}_{fg} \frac{d\underline{v}_{Kg}}{dt} = \dot{\underline{v}}_{Kf} + \underline{\Omega}_f \times \underline{v}_{Kf} \tag{6}$$

and the assumption, that \dot{q} is equal to zero, we get the equations for the quasi-stationary 2D-model:

$$\begin{aligned}
 0 &= \Sigma X_f - m \cdot (g - \dot{w}_{Kg}) \cdot \sin \theta - \dot{u}_{Kg} \cdot \cos \theta \\
 0 &= \Sigma Z_f + m \cdot (g - \dot{w}_{Kg}) \cdot \cos \theta - \dot{u}_{Kg} \cdot \sin \theta \\
 0 &= \Sigma L_f \\
 0 &= \Sigma M_f \\
 0 &= \Sigma N_f
 \end{aligned} \tag{7}$$

The fundamental advantage of these equations is, that they can be solved iteratively for predetermined geodetical accelerations. This corresponds to a predetermination of the flight path. Iterative variables for instance are the four control inputs and the pitch angle.

The equilibrium of power has to be satisfied as an further equations:

$$0 = P_{req.} - M_R \cdot \omega_R - M_{TR} \cdot \omega_{TR} - P_{aux.} \quad (8)$$

Consequently, there are in total six iteration variables. The complete iterative solution of the equations at any time step of simulation is stated here as "implicite" simulation. Table 1 gives a survey on a selection of possible combinations of the iteration variables.

	$\vartheta_{O,R}$	ϑ_s	ϑ_c	$\vartheta_{O,TR}$	θ	q	\dot{q}	u_{Kg}	\dot{u}_{Kg}	w_{Kg}	\dot{w}_{Kg}	$P_{req.}$
1	x	x	x	x	x							x
2	x	x	x	x	x				x			
3		x	x	x	x				x			x
4	x	x	x	x	x						x	
5			x	x	x				x		x	x

Table 1 Selection of Potential Iteration Variables (x)

With case 1 the translational geodetical accelerations are predetermined analytically as ideal functions of time. Here the translational velocities as well as the flight path are known from the integration. Case 2 comprises the predetermination of the vertical geodetical acceleration and power available. Apart from the control inputs, the pitch angle and the horizontal acceleration capability are iterated. Different to case 2, with case 3 the collective pitch is predetermined instead of power available. Although the conditions are quite similar, there occur little differences concerning the flight path. Constant power means only approximately constant collective pitch. Analogous to case 2, case 4 contains the predetermination of the horizontal degree of freedom and power available. The results are the control inputs, the pitch angle and the vertical degree of freedom, e.g. the vertical acceleration capability.

For first optimization calculations without knowing the optimum, the quasi-stationary 2D-model is only suitable to a limited use because of computation time. As a further physical simplification of the model, equations (7), will not be permissible, one has to consider the simplification of the numerical solution. These considerations result in a quasi-stationary data field model basing on stationary performance calculations.

3.4 Quasi-Stationary Data Field Simulation Model

The data fields contain power required of the helicopter as a function of gross weight, atmospheric conditions and flight state. As flight states, stationary horizontal and vertical motions with

and without ground effect are taken into account. For building up the data fields, data reduction methods from /10/ are used decreasing the number of independent variables.

Since during takeoff and landing procedures there occur accelerated flight states which are not directly considered in the data fields, accelerated states have to be transformed into equivalent stationary states. It can be shown that translationally-accelerated and the corresponding stationary states are equal in control input, inflow angle and power required. This applies to the simplifications leading to equations (7). The accelerated flight can be transformed into a stationary flight at same velocity, but different gross weight and flight path angle.

Again, it should be noted, that the data field model physically corresponds to the quasi-stationary 2D-model and does not contain further simplifications.

The calculation of the flight state variables, power required, respectively, is performed by means of multi-dimensional spline interpolation. Another possibility would be to describe the data fields by multi-dimensional polynomials. The computation time for a takeoff or landing simulation is reduced by the factor >10 when using the data field model, excluding the time required for establishing the data fields. The data fields can either be established on the basis of performance calculation, for instance by the quasi-stationary 2D-model, or on the basis of flight tests.

The non-dimensional hover diagram is presented in figure 8. It takes into account the influence of gross weight and atmospheric conditions. We do not want to go into details regarding reduction of power required and independent state variables as described in /10/. Figure 9 shows a typical data field in reduced form resulting from performance calculations. A power factor as a function of non-dimensional horizontal and vertical velocities is shown. The diagram demonstrates the power factor for a certain height OGE. For different ground effect heights corresponding surfaces will be obtained.

The accordance of the simulation results achieved by the quasi-stationary 2D-model and by the data field model only depends on the number of data points representing the data field. It was found out that a performance calculation in steps of $u_{Kg}=5\text{m/s}$ and $w_{Kg}=1\text{m/s}$ is sufficient. During the simulation by means of the data field model it is important to pay attention to the fact that the flight envelope for which the data field is valid, must not be left. On principle, only an interpolation within the data field is permitted, extrapolation is not allowed.

4. Results

4.1 Comparison of Three-Dimensional and Quasi-Stationary Two-Dimensional Simulation

The admissibility of the simplifying assumptions which lead to the quasi-stationary simulation has to be examined. One possibility is the simulation of selected takeoff and landing maneuvers by means of the 3D- and the quasi-stationary 2D-model. It is a matter of course that here only the influence of the simplifications can be shown which lead from the 3D-model to the quasi-

stationary 2D-model. The advantage of the theoretical comparison in opposition to the experimental comparison by means of flight tests is to be seen in the exact reproducibility of boundary conditions, for instance of atmospheric conditions.

Apart from a detailed description of the 3D-simulation reference /11/ states results for different maneuver calculations, among others some results for takeoff and landing simulations. We do not want to enter into the particulars of the problems regarding controllability, automatic control system, pilot model, respectively. It should be noted that in /11/ was not carried out an optimization of the automatic control system, and a flight path control system was not realized.

Figure 10 presents the results from the 3D- and the quasi-stationary 2D-simulation of a normal takeoff with constant collective. As a boundary condition for comparing calculations the exact accordance of the flight path was chosen. The geodetical accelerations of the longitudinal motion and this way also the velocities as well as the flight path from the 3D-simulation have been predetermined in the quasi-stationary simulation. The influence of the simplifications then occurs for example in power required, pitch angle and control inputs. The accordance of pitch angle and power required is very good. No differences can be seen in pitch angle. Angular velocities and accelerations have only a small influence on power required. Therefore neglecting angular velocities and angular accelerations of the lateral motion and the assumption of a quasi-stationary degree of freedom in pitch is permitted.

Considering the control inputs, also the constant collective pitch of the main rotor is excellently reproduced by the quasi-stationary model. Differences occur at the cyclic pitches and the collective pitch of the tail rotor in regions with a strong dynamic in pitch. These differences can mainly be explained by the neglect of rate and acceleration of pitch in the moment equations of the quasi-stationary model. The principle course and the final stationary values of the control inputs are represented very well by the quasi-stationary 2D-model.

Due to these excellent results a further point of view regarding the general simulation of takeoff and landing procedures should be noted. The control inputs as calculated from the quasi-stationary 2D-simulation can be used as feed-forward commands for the 3D-model in support of a simple additional feed-back controller, a simple pilot model, respectively. In /12/ a similar method is reported. Recent simulation studies show promising results following a predetermined flight path without an explicit flight path control concept. In context with the optimization the 3D-simulation is of interest proving the ability to fly optimized maneuvers.

4.2 Comparison of Flight Test and Quasi-Stationary Two-Dimensional Simulation

The admissibility of simplifying assumptions already contained in the 3D-model could not be checked in the theoretical comparison. These are for instance the assumptions of a stationary aerodynamic and a stationary engine. A further checking of the quasi-stationary simulation has to be realized by the comparison with flight tests.

The normal procedures of takeoff and landing were performed by flight tests with the helicopter BO 105. Apart from the flight state variables digitally recorded on board the flight path was recorded by a LASER-Tracking-System on ground.

Although takeoff and landing investigations are mainly concerned with the determination of takeoff and landing distances, the flight path and thus the velocities and accelerations of the flight test are predetermined in the quasi-stationary simulation. This procedure was chosen in order to be able to compare directly power required calculated from simulation with power required from flight tests.

Figure 11 shows the comparison of calculation and flight test for a normal takeoff. The horizontal and vertical distances, the pitch angle and power required are demonstrated. The pitch angle shows good accordance between flight test and simulation. Also power required is stated adequately in the simulation. The quasi-stationary simulation model calculates power required for hover IGE at the beginning of takeoff equal to power required confirmed by the flight test. There are slight power differences in certain sections.

In the quasi-stationary simulation model a stationary rotor is considered at any time step and the induced velocities at the rotor disc are determined by a stationary inflow calculation. Dynamic effects as for instance a small variation of rotor speed or an acceleration of the mass flow through the rotor were not taken into consideration. The ground vortex has a further effect on power required which is not considered in the source model. Moreover, the source model does not take into account the effect of the pitch angle in ground effect. It is indeed possible to extend the source model to this effect, however, there do not exist experimental studies for verification. Ground effect investigations for forward flight have to prove the validity of the source model.

Figure 12 and 13 present results from the quasi-stationary simulation for a Cat. A takeoff procedure with engine failure within the CDP. A typical continued takeoff is shown in figure 12. At first, the helicopter accelerates IGE without height loss and changes into climb after reaching a velocity of $V=45$ kts. Within the critical decision height H_{CDP} one engine fails. The power of the operating engine is increased to 93% emergency power for continued takeoff and the helicopter performs a safe climbout. The 50ft-height is dynamically exceeded in transition.

The rejected takeoff after engine failure can be taken from figure 13. Contrary to the continued takeoff, the power of the operating engine is strongly reduced to allow the helicopter to change from climb into descent. Here also the helicopter reaches the 50ft-height dynamically. After descent the flare is performed. It is only during this maneuver that the 93% emergency power is needed. During the flare the forward velocity is not completely reduced and the helicopter touches down with a remaining velocity.

The takeoff and landing distances given in the flight-manual of the BO 105 compared to the results of the quasi-stationary simulation show good agreement. The data of the manual base on flight tests of the manufacturer verified for certification.

Concerning the Cat. A procedure no own flight tests were performed.

4.3 Effects on Takeoff and Landing

Atmospheric conditions, takeoff weight, power available as well as maneuver-strategy have an important effect on takeoff and landing flight path. These effects will be discussed for normal takeoff and continued takeoff maneuver of Cat. A procedures. For calculations the quasi-stationary simulation model is used. The twin-engine helicopter BO 105 is chosen as example.

Figure 14 demonstrates the effect of takeoff weight on flight path for Cat. A continued takeoff. As expected, increasing takeoff weight leads to an increasing takeoff distance. It is supposed that one engine fails in a height of $H=10m$. It can be clearly seen that the climb will take place later when the weight is increased. This results from a less power excess ensuing a less horizontal acceleration capability. In all three cases the final velocity is the same. The maximum flight path angle will be reached later and is significantly decreased at increased weight due to a reduced climb capability.

Figure 15 shows the effect of different engine power available, takeoff power, respectively, for Cat. A continued takeoff. The takeoff power mainly effects the horizontal acceleration segment, when the takeoff power is already reached before the climb segment. An increase of the takeoff power leads to a decrease of the horizontal acceleration segment. Within the climb segment there are only small differences in flight path. The reason is to be found in higher horizontal acceleration at the beginning of the climb due to increased takeoff power. In all cases the horizontal acceleration is reduced by the same gradient so that for increasing takeoff power there occur higher horizontal velocities and higher climb velocities. The flight path angle does only slightly change.

The maneuver strategy has an essential effect on the flight path. Figure 16 demonstrates for one gross weight and one determined takeoff power the influence of the horizontal acceleration gradient by which the horizontal acceleration is reduced at the beginning of the climb segment. At increasing gradient the flight path angle in the climb segment will be increased and the takeoff distance up to reaching the 50ft-height is significantly decreased. By reducing the horizontal acceleration more quickly, the maximum vertical acceleration will be reached earlier. The flight path angles do not show important differences after engine failure. With increasing gradients the decrease of takeoff distances gets smaller.

It is notable in figures 14 to 16 that after engine failure there do not occur any negative flight path angles. A climb is possible at all times, whereas in the segmental division according to figure 1 a descent region has been supposed. This results as well from a chosen airspeed at the time of engine failure, for which the helicopter is in a favourable range of power required, as from a high remaining power available of the operating engine. There may indeed be the possibility that after

engine failure the helicopter first has to be accelerated horizontally in order to get into a favourable flight region. This way there occur flight paths, as shown in figure 1.

The effect of the maneuver strategy as already hinted in figure 16 shall be discussed more in detail for a normal takeoff without engine failure. Figures 17 to 20 show the results for a helicopter with small power excess, which cannot hover OGE. Different horizontal acceleration maneuvers were investigated.

Figure 17 shows the takeoff IGE from a skid height of $H_{IGE}=1m$ with constant collective pitch, i.e. at nearly constant P_{IGE} power required, maneuver I. If the helicopter accelerates horizontally a simultaneous loss in height will be inevitable under this condition. Up to a horizontal acceleration of $\dot{u}_{Kg}=1m/s^2$ there will not be ground contact. At smaller acceleration shorter takeoff distances can be reached. In all cases the final velocity amounts to $u_{Kg}=20m/s$. It will not partly be reached within the range of $x_g=300m$.

From figure 18 one can take the maneuver II which is in principles the same as maneuver I. However, takeoff begins at a skid height of $H_{IGE}=2m$ with a higher collective pitch. Here also the collective pitch is kept constantly. A horizontal acceleration of $\dot{u}_{Kg}=1,8m/s^2$ is the maximum acceleration, enabling a takeoff without ground contact. Considering the takeoff distance up to reaching a height of $H=15m$, it can be clearly seen that smaller accelerations are more advantageous. The shortest takeoff distance is obtained within the range of $\dot{u}_{Kg}=0,6m/s^2$.

Figure 19 shows the takeoff from hover at $H_{IGE}=1m$, maneuver III. An increase of the collective pitch to a value P_{IGE} corresponding to the hover IGE at $H_{IGE}=2m$ (collective pitch of the maneuver II in figure 18) is allowed. The collective pitch is increased within 2s. Now it can be demanded that there is no height loss during horizontal acceleration. In this maneuver there will be accelerated with maximum possible horizontal acceleration in ground effect up to different final velocities u_{Kg} for afterwards rotating in climb. A favourable flight path with minimum takeoff distance is seen at a final velocity within the range of $u_{Kg}=10m/s$. As the ground effect has been considerably reduced within $u_{Kg}=10$ to $15m/s$, an acceleration exceeding this range will not take any advantage from ground effect. The flight path for $u_{Kg}=5m/s$ shown in figure 19 is interesting. At this velocity the helicopter has only the capability of a horizontal flight IGE.

Figure 20 contains a comparison of different maneuvers I, II and III. Moreover, an additional maneuver is shown ($\dot{u}_{Kg}=0,6m/s^2$, $u_{Kg}=12m/s$). The flight path I represents the takeoff at lowest level of power, thus having the longest takeoff distance. For the remaining maneuver the power required for hover at $H_{IGE}=2m$ is available as maximum power. The takeoff distance up to reaching a height of $H=15m$ is chosen for rating. Maneuver II, takeoff with constant collective pitch at $H_{IGE}=2m$, will be more favourable than maneuver III, takeoff with increasing collective pitch and horizontal acceleration maneuver without height loss, for reaching a final velocity $u_{Kg}=20m/s$. Up from a height of $H=23m$ maneuver III will be more advantageous. For reaching a final velocity of $u_{Kg}=12m/s$ leading to a small takeoff distance as already shown in figure 19, maneuver III shows clearly an advantage to maneuver II.

Maneuver III takes profit from the influence of ground effect at a lower height.

The maneuvers stated here are important pre-investigations for later optimizations. By means of parameter variation the essential effects on takeoff and landing can be studied. In /3/ similar takeoff maneuvers as shown in figure 19 are examined. However, in that case a constant horizontal acceleration within the horizontal acceleration segment has been supposed.

5. Conclusion

Takeoff and landing procedures of helicopters according to FAR Part 27 and FAR Part 29, Cat. A und B, have been presented and prepared for the numerical simulation. For this purpose a maneuver-orientated segmental division has been established.

Based on a three-dimensional simulation model considering the complete longitudinal and lateral motion of the helicopter, a quasi-stationary two-dimensional simulation model has been developed. As both the models are only to a limited extent suitable for optimization investigations due to computation time, a quasi-stationary simulation basing on stationary data fields, a so-called data field model, has been proposed. The data field model does not contain any further physical simplifications compared to the quasi-stationary model, however it needs considerable less computation time. In the simulation models the ground effect is considered by a modified source model.

The comparison of results from the three-dimensional and quasi-stationary two-dimensional simulation shows a very good accordance. So the allowability of the simplifying assumptions which lead to the quasi-stationary model can be regarded as confirmed. The influence of angular velocities and accelerations on power required can be neglected. Furthermore, the results from the quasi-stationary simulation have been confirmed by flight tests with a BO 105 helicopter for a normal takeoff. In case of Cat. A takeoff with engine failure, the simulation results show good agreement with data from the helicopter flight manual.

The essential variables effecting takeoff and landing procedures have been discussed. Apart from gross weight, atmospheric conditions and power available the maneuver strategy has an important effect on the flight path. Different maneuver strategies have been presented for normal takeoff with the example of a helicopter which cannot hover out of ground effect due to an assumed maximum takeoff power. Using the ground effect will not be of advantage in any case as far as shorter takeoff distances are concerned. It can be taken from the results that parameter studies regarding maneuver strategy are essential especially for further optimization investigations.

For modification of the quasi-stationary model there are different approaches which can be taken into consideration. Concerning the ground effect the influence of pitch angle and the ground vortex has to be estimated. The source model can be extended to the effect of the pitch angle. It has to be checked, how far the ground vortex can be described by a simple approximative approach. Meanwhile, the extension of the engine model to a dynamic engine simulation has been started. For this purpose a corresponding

engine control system has been designed. Further investigations have to find out whether the engine dynamic is relevant for take-off and landing performances.

Optimization of takeoff and landing performances, especially for Cat. A procedures, are planned for the near future. The optimization calculations will be performed by means of the quasi-stationary data field model. The parameter studies regarding maneuver strategy for normal takeoff as well as the results for the Cat. A procedures demonstrate that there does exist a large range of possible procedures at predetermined helicopter performance capability. This leads to the conclusion that compared with the present procedures there may be developed significantly improved takeoff and landing procedures.

Acknowledgement

The paper is based on research work funded by the Deutsche Forschungsgemeinschaft DFG under SFB 212 "Sicherheit im Luftverkehr".

6. References

- /1/ U.S. Department of Transportation, Federal Aviation Administration, Federal Aviation Regulations, Part 27 - Airworthiness Standards: Normal Category Rotorcraft, 1972
- /2/ U.S. Department of Transportation, Federal Aviation Administration, Federal Aviation Regulations, Part 29 - Airworthiness Standards: Transport Category Rotorcraft, 1974
- /3/ F.H. Schmitz, Take Off Optimization for STOL Aircraft and Heavily Loaded Helicopters, Res. and Dev. Techn. Rep. ECOM-02412-4, Aug. 1969
- /4/ T. Cerbe, Ein quasistationäres Rechenmodell mit Berücksichtigung des Bodeneffektes zur Simulation von Start- und Landevorgängen von Hubschraubern, DGLR Jahrestagung, Votr.-Nr.:086-152, 1986
- /5/ H. Huber, G. Polz, Helicopter Performance Evaluation for Certification, 9th European Rotorcraft Forum, Pap. No.: 26, 1983
- /6/ I.C. Cheeseman, N.E. Bennett, The Effect of the Ground on a Helicopter Rotor in Forward Flight, AAEE Report, Rep. and Mem. No. 3021, 1955
- /7/ T. Cerbe, Zum Bodeneffekteinfluß auf Schub und Leistungsbedarf eines Hubschraubers, DGLR-Jahrestagung, Poster-Nr.: 085-175, 1985
- /8/ H.C. Curtiss Jr. et.al., Rotor Aerodynamics in Ground Effect at Low Advanced Ratios, 37th Forum of the American Helicopter Society, 1981
- /9/ P.F. Sheridan, W. Wiesner, Aerodynamics of Helicopter Flight near the Ground, 33rd Forum of the American Helicopter Society 1977
- /10/ K. Liese, J. Russow, G. Reichert, Correlation of Generalized Helicopter Flight Test Performance Data with Theory, 13th European Rotorcraft Forum, Pap. No.:7.6, 1987
- /11/ U. Arnold, Entwicklung einer Hubschraubersimulationsprogrammes, DGLR Jahrestagung, Votr.-Nr.: 087-123, 1987
- /12/ G.A. Smith, G. Meyer, Aircraft Automatic Flight Control System with Model Inversion, Journal of Guidance Vol.10 No.3, 1987

7. Appendix

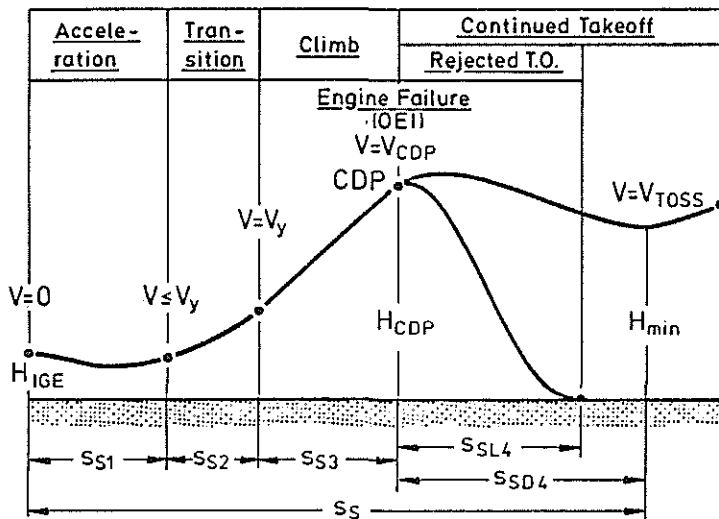


Figure 1 Segments for Cat. A-Takeoff

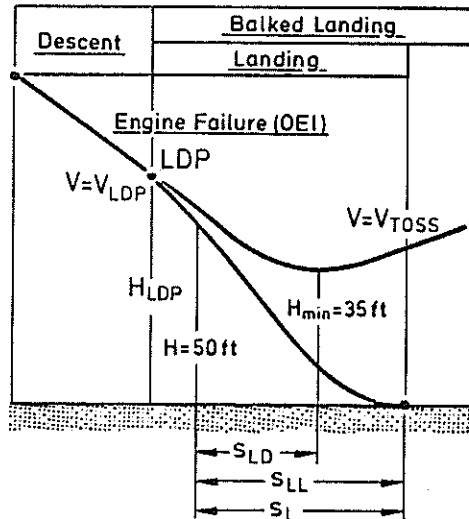


Figure 2 Segments for Cat. A-Landing

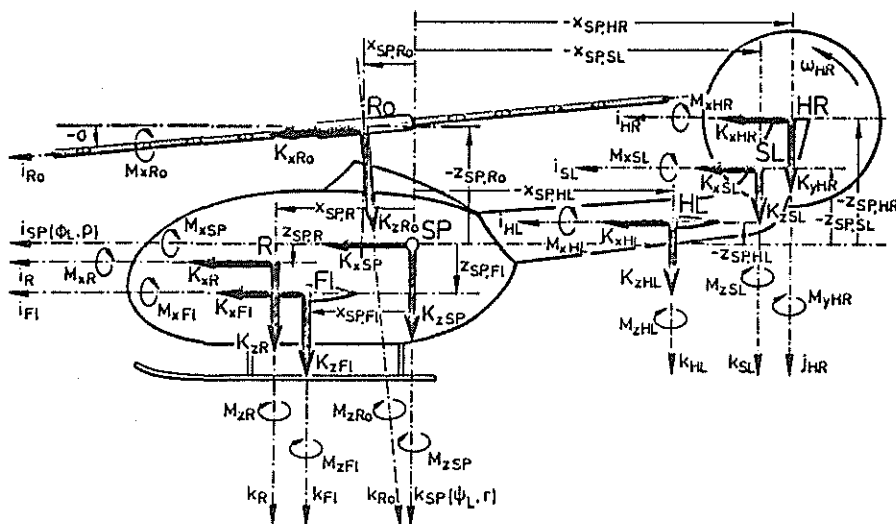


Figure 3 Helicopter Forces and Moments

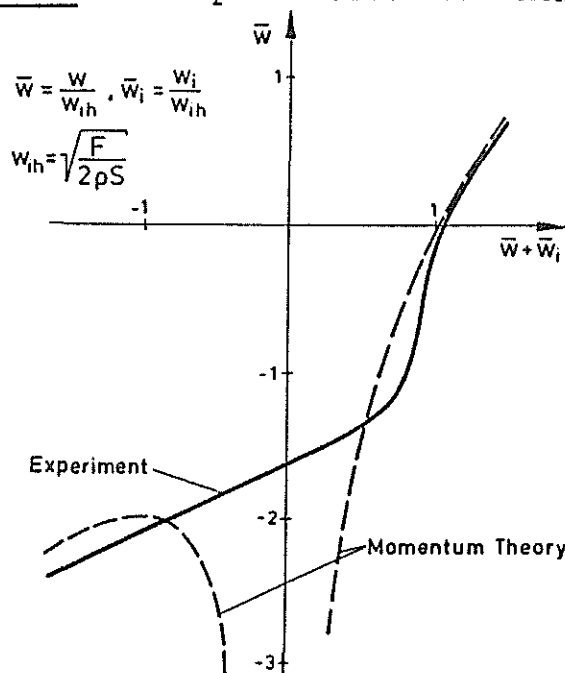


Figure 4 Induced Velocity from Momentum Theory versus Experiment

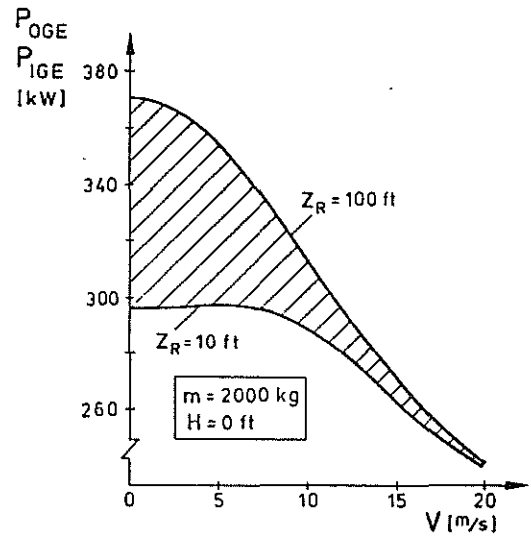
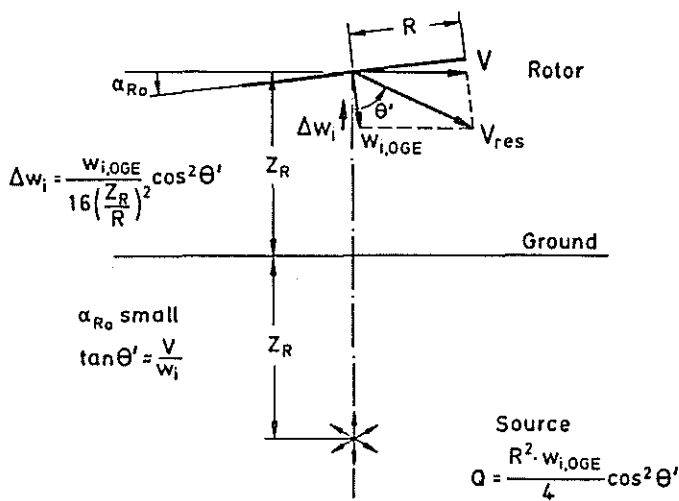


Figure 5 Source Model in Forward Flight

Figure 6 Decrease in Power Required due to Ground Effect

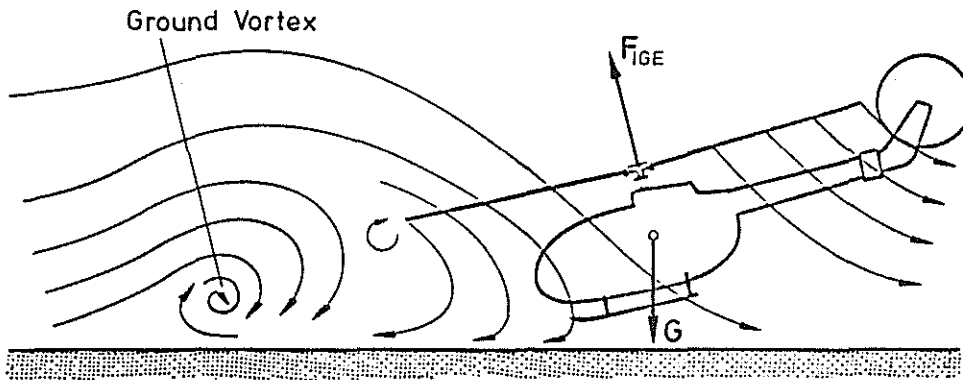


Figure 7 Helicopter in Ground Effect for Low Forward Speed

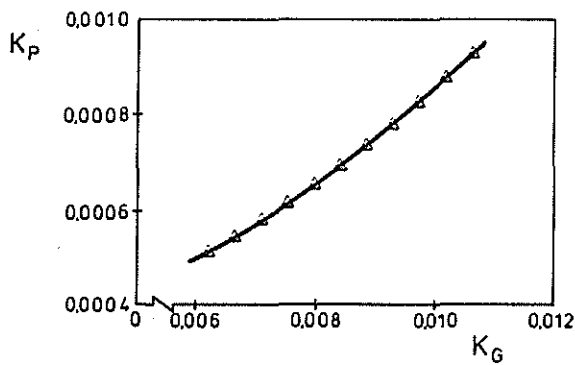


Figure 8 Non-Dimensional Power Required for Hover OGE

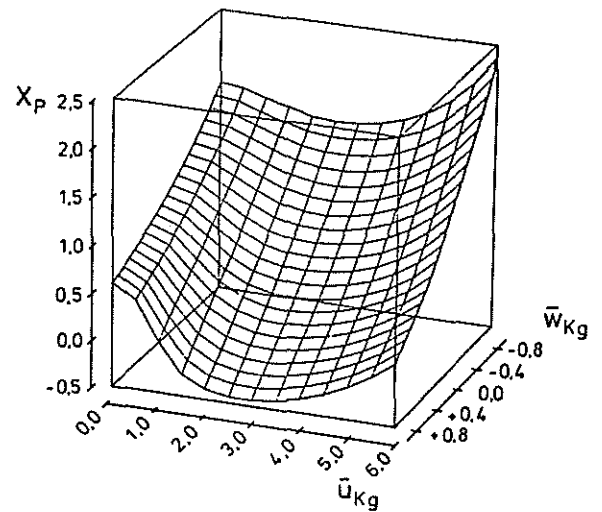


Figure 9 Power Factor at Forward Flight with Climb/Descent

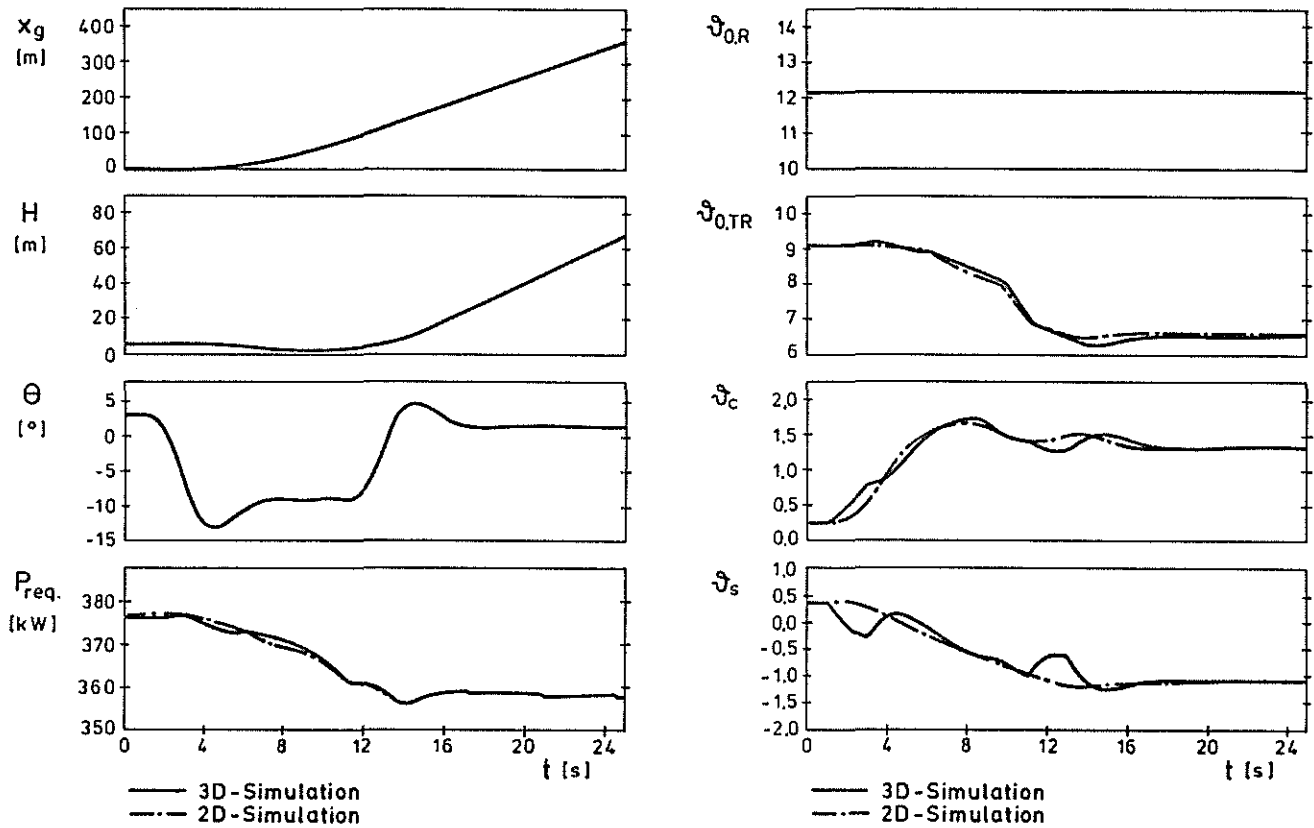


Figure 10 Normal Takeoff from 2D-/3D-Simulation

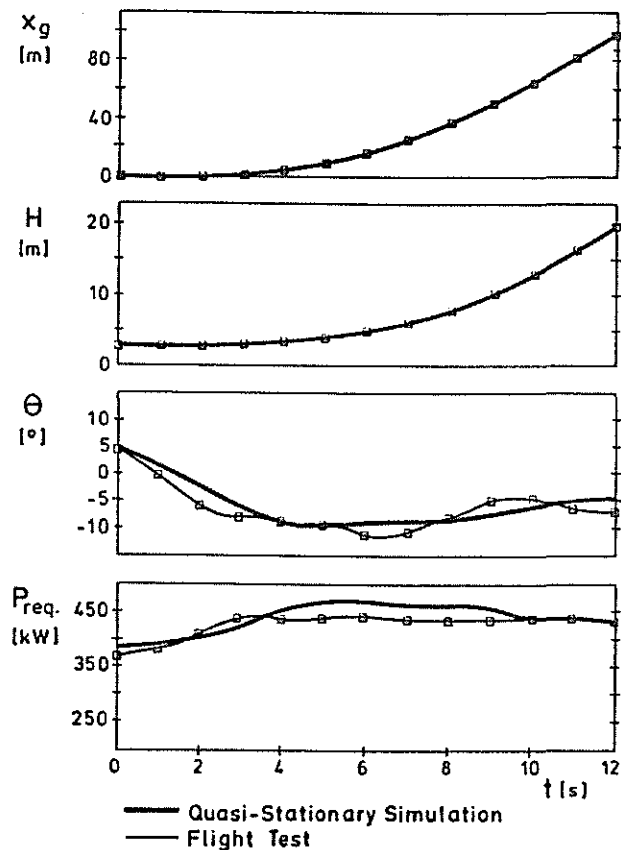


Figure 11 Normal Takeoff from Simulation/Flight Test

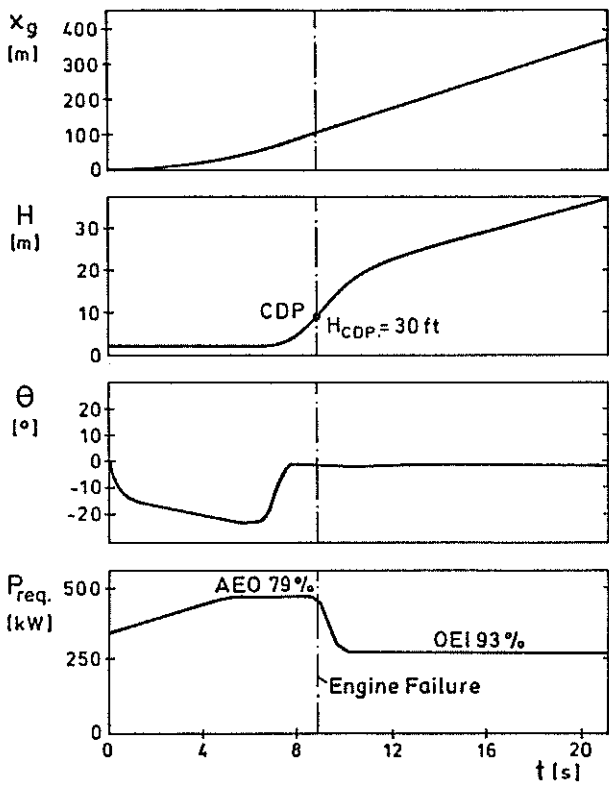


Figure 12 Cat.A-Continued Takeoff

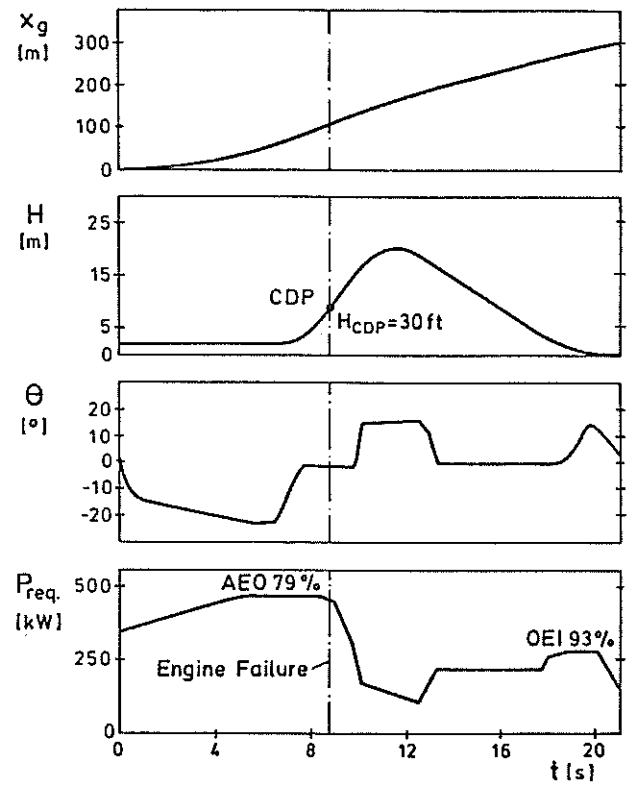


Figure 13 Cat.A-Rejected Takeoff

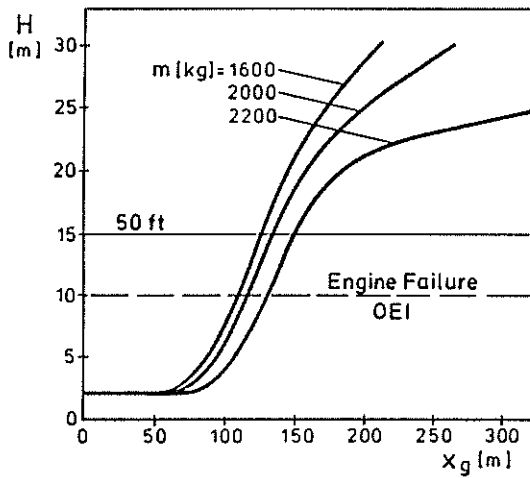


Figure 14 Effect of Gross Weight
Cat.A-Continued Takeoff

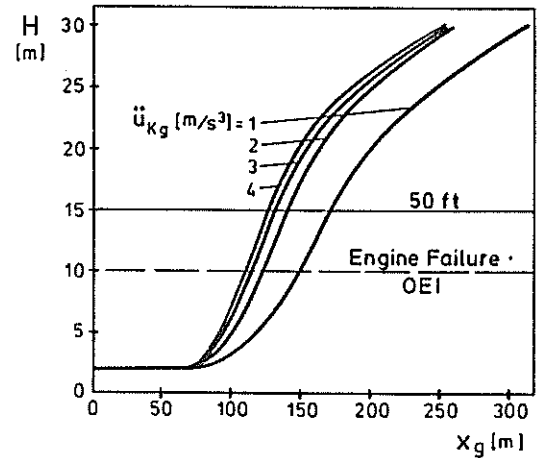


Figure 16 Effect of Horizontal
Deceleration, Cat.A-
Continued Takeoff

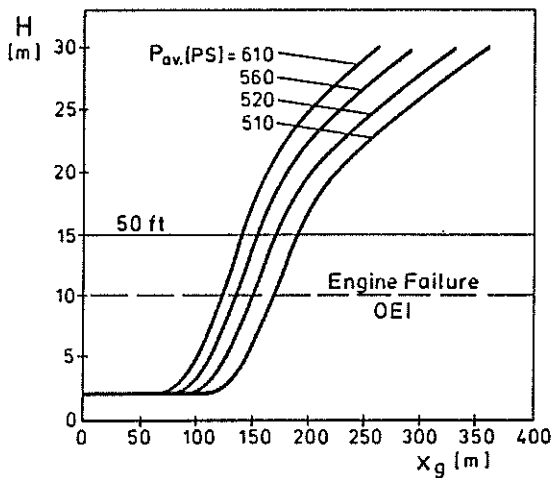
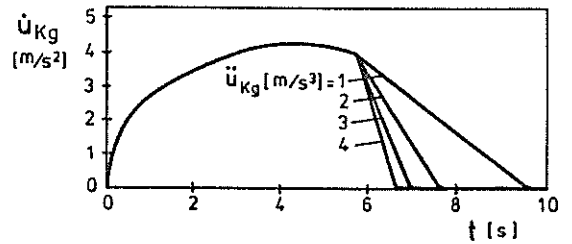


Figure 15 Effect of Power Available
Cat.A-Continued Takeoff



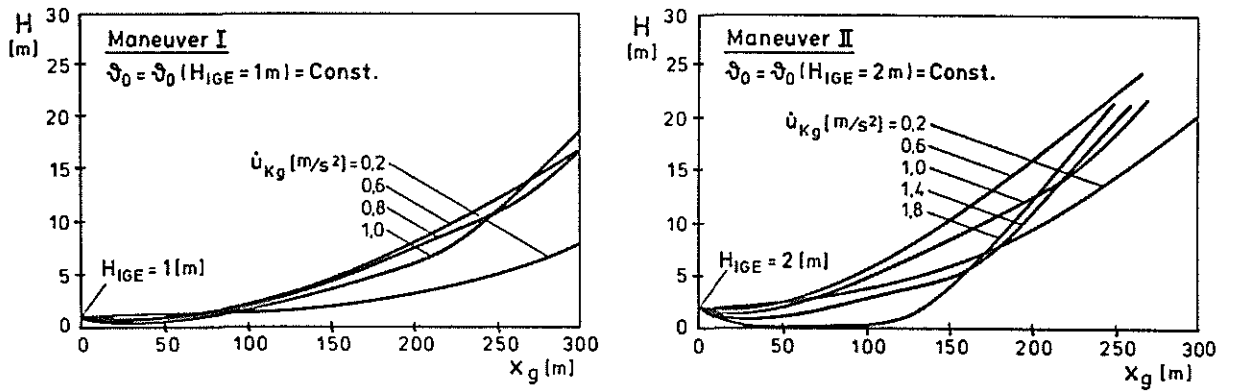


Figure 17-18 Effect of Maximum Horizontal Acceleration Takeoff with Constant Collective

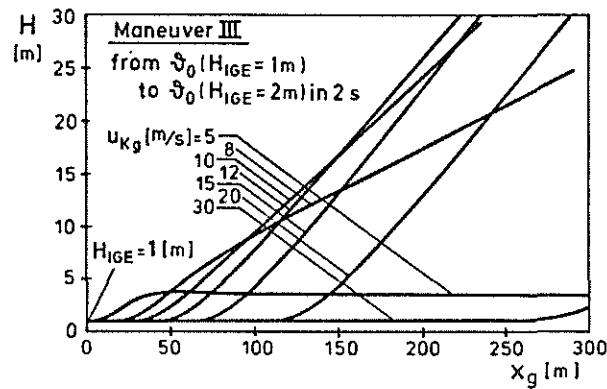


Figure 19 Effect of Maximum Speed to Accelerate Takeoff without Height Loss

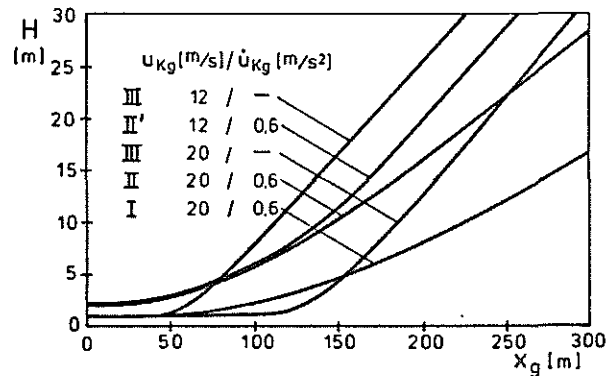


Figure 20 Comparison of Takeoff Maneuvers I, II, III